Published in final edited form as:
Invest Ophthalmol Vis Sci. 2008 March ; 49(3): 1048–1055.

Role of Carbonic Anhydrase IV in Corneal Endothelial HCO_3^- Transport

Xing Cai Sun, **Jinhua Li**, **Miao Cui**, and **Joseph A. Bonanno**

Abstract

Purpose—Carbonic anhydrase activity has a central role in corneal endothelial function. Here, we examined the role of CAIV in facilitating CO_2 flux, HCO_3^- permeability, and HCO_3^- flux across the apical membrane.

Methods—Primary cultures of bovine corneal endothelial cells were established on membrane permeable Anodiscs. Apical CAIV was inhibited by benzolamide or siRNA knockdown of CAIV. Apical CO_2 fluxes and HCO_3^- permeability were determined by measuring pH_i changes in response to altering the CO_2 or HCO_3^- gradient across the apical membrane. Basolateral to apical HCO_3^- flux was determined by measuring the pH of a weakly buffered apical bath in the presence of basolateral bicarbonate rich ringer. In addition, we measured the effects of benzolamide and CAIV knockdown on steady-state ΔpH (apical - basolateral compartment pH) after four hours incubation in DMEM.

Results—CAIV expression was confirmed and CAIV was localized exclusively to the apical membrane by confocal microscopy. Both 10 μM benzolamide and CAIV siRNA reduced apparent apical CO_2 fluxes by ~20%, however they had no effect on HCO_3^- permeability or HCO_3^- flux. The steady-state apical-basolateral pH gradient at four hours was reduced by .12 and 0.09 pH units in benzolamide and siRNA treated cells, respectively, inconsistent with a net cell to apical compartment CO_2 flux.

Conclusions—CAIV does not facilitate steady-state cell to apical CO_2 flux, apical HCO_3^- permeability or basolateral to apical HCO_3^- flux. The steady-state pH changes however, suggest that CAIV may have a role in buffering the apical surface.

Keywords

corneal endothelium; Carbonic Anhydrase IV; CO_2 Flux; HCO_3^- Flux

Introduction

Carbonic anhydrase activity has a central role in corneal endothelial function. Several laboratories [1-4] have consistently shown that rabbit corneas mounted in vitro in a Dikstein-Maurice type chamber swell in response to direct application of carbonic anhydrase inhibitors (CAIs) to the endothelial surface. Clinically, topical use of CAIs generally do not affect normal corneas presumably due to the much lower concentration of drug at the endothelial surface [5-9]. However, topical CAIs can cause corneal edema in corneas with low endothelial cell density [10, 11], suggesting that there is a threshold reserve of carbonic anhydrase activity or that inhibition of CA activity has a greater impact when other endothelial properties (e.g., barrier function) are compromised. There are at least two CA isoforms expressed in corneal

Corresponding author: Joseph A. Bonanno, Indiana University, School of Optometry, 800 E. Atwater Ave., Bloomington, IN 47405, Tel: 812-856-5977, Fax: 812-855-7045, Email: jbonanno@indiana.edu.

Commercial relationships: None

endothelium, the cytosolic CAII [12-14] and the membrane bound CAIV [15-17]. SAGE analysis suggests that another membrane isoform, CAXII, is also expressed [18].

The sensitivity of corneal endothelial fluid transport to CAIs and the abrogation of fluid transport in the absence of HCO_3^- [1, 2, 19] have led to the notion that endothelial fluid transport is due to transport of HCO_3^- that is facilitated by CA activity. All carbonic anhydrases significantly speed the hydration and dehydration of CO_2. At membrane interfaces CA activity can facilitate net CO_2 flux [20] and transport of HCO_3^- [21, 22]. Recent studies have suggested that HCO_3^- transporters can form complexes with CAII or CAIV (transport metabolons) and facilitate HCO_3^- fluxes by rapid conversion to CO_2 thereby maximizing local HCO_3^- gradients [23-25]. CAIs also produce acidosis consistent with their contribution to HCO_3^- buffering capacity [26, 27], and in corneal endothelium application of acetazolamide, a cell permeant CAI, reduces intracellular pH (pH_i) [28]. The mechanism(s) by which CA activity contributes to corneal endothelial function, by facilitating CO_2 flux, HCO_3^- flux, or buffering capacity, however is unknown.

Most readily available CAIs are cell permeant and inhibit all CA isoforms. One recent study [29] however, has shown that the relatively impermeant CAI, benzolamide, and a dextran linked CAI can cause swelling of rabbit corneas in vitro at about half the rate of cell permeant CAIs, indicating that CAIV and CAII have additive functions. Benzolamide applied to the apical surface of corneal endothelial cells can slow apical CO_2 fluxes that is reversed by addition of CA to the bath [30]. These results suggested that CO_2 diffusion from cell to apical surface, followed by conversion to HCO_3^- (facilitated by CAIV), could contribute to net HCO_3^- transport, but does not show that this process actually occurs.

In this study we examined the role of CAIV in apical CO_2 flux, apical HCO_3^- permeability, basolateral to apical HCO_3^- flux, and steady-state bath pH changes across cultured bovine corneal endothelium by comparison of these parameters with benzolamide or CAIV siRNA treated monolayers. The results indicate that CAIV does not have a role in net CO_2 flux, apical HCO_3^- permeability or HCO_3^- flux and suggest that CAIV may function to buffer the apical surface.

MATERIALS AND METHODS

Cell culture

Bovine corneal endothelial cells (BCEC) were cultured to confluence onto 25-mm round coverslips, 13-mm Anodisc filters, Anopore tissue culture inserts or T-25 flasks as previously described [31]. Briefly, primary cultures from fresh cow eyes were established in T-25 flasks with 3 ml of Dulbecco's modified Eagle's medium (DMEM), 10% bovine calf serum, and antibiotic (penicillin 100U/ml, streptomycin 100 U/ml, and Fungizone 0.25 μg/ml), gassed with 5 % CO_2-95% air at 37 °C and fed every 2 to 3 days. Primary cultures were subcultured to three T-25 flasks and grown to confluence in 3 to 5 days. The resulting second passage cultures were then further subcultured onto coverslips, Anodiscs or Anopore inserts and allowed to reach confluence within 5 to 7 days.

RT-PCR screening

mRNA was extracted and purified from fresh and cultured BCEC as well as bovine lung, using the Oligotex mRNA mini kit from Qiagen as per manufacturer's protocol. The purified mRNA was then used for cDNA synthesis and CAIV PCR. cDNA synthesis was performed using Invitrogen Superscript III (200U/ul), Oligo dT_{12-18} primer and 1 ug mRNA as previously described [32]. 100 μL of CAIV PCR was performed in an Expand High Fidelity PCR reaction buffer (Roche) with 0.5 μL Taq polymerase (Roche), 5 μL of cDNA template, 8 μL of dNTP

mix (2.5 mM each) and 0.3 μM (final concentration) CAIV primers. The PCR parameters are denaturation at 94°C for 3 min for one cycle, 30 cycles of denaturation at 94°C for 30 seconds each, annealing at 50-60°C for 1 min, extension at 71°C for 2 min, and a final extension for one cycle at 71°C for 10 min. The PCR products were separated on 1.7% agarose electrophoresis gels and stained with 0.5μg/mL ethidium bromide. Water and no RT controls were routinely added. CA IV primers: product length: 468 bp, CA IV sense: 5′-TGCTACCAGATTCAAGTCAAGCCTTC-3′, CA IV antisense: 5′-AAGTTCACATTCTTGGATCCGTCCAC-3′. The expected PCR bands were excised from the agarose gel, purified using a Qiagen gel purification kit, subcloned into pCR-TOPO downstream from a T7 sequence, and transformed into One Shot Chemically Competent E. coli. This plasmid was submitted to the Biochemistry Biotechnology Facility, Indiana University School of Medicine, Indianapolis, for sequencing. Confirmation of our PCR results was obtained by comparison of the sequence results using BLAST software (NCBI) against the NCBI database.

siRNA Transfection

The siRNA construction and treatment was performed as previously described [32-35]. Briefly, several sense and anti-sense sequences corresponding to CAIV cDNA were designed and blasted by using the Ambion siRNA targeting design tool and were purchased from Invitrogen. Using these oligonucleotides, four 21-nucleotide siRNAs for CAIV were synthesized using the Silencer siRNA construction kit from Ambion. We found that target sequence 120-140 of the CAIV ORF, 5′- AAGTCAAGCCTTCCAACTACA -3′ antisense and 5′-AATGTAGTTGGAAGGCTTGAC sense was most effective at 20 nM, 3-4 days post-transfection. A siCONTROL non-targeting siRNA (no known mammalian homology) was purchased from Dharmacon. Cells were transfected when 70-80% confluent using Oligofectamine (Invitrogen) according to the manufacturer's protocol in the presence of siRNA. Cells were incubated with 1 ml OPTI-MEM I (Gibco) containing siRNA for four hours followed by addition of 2 ml of standard DMEM with serum. T-25 flasks were treated with 2 ml OPTI-MEM I containing siRNA followed by addition of 4 ml of culture media. Media was then changed every 2 days.

Immunoblotting

Total membrane protein was extracted from fresh and cultured BCE using the sulfo-NHS-biotin technique, as previously described [36]. Cultured and fresh bovine corneal endothelial surface proteins were labeled with 200 μg of EZ-link sulfo-NHS-biotin (Pierce) per mL of bicarbonate free ringer, pH 7.5, at room temperature for 30 minutes. The cells were lysed (50 mM Tris base, 150 mM NaCl, 0.5% deoxycholic acid-sodium salt, 2% SDS and 1% NP-40, pH7.5 protease inhibitor cocktail), and then sonicated. This was followed by centrifugation at 10,000 rpm to pellet cell debris. The supernatant was incubated with 50 μL of immobilized streptavidin at 4°C for overnight, rotated end over end. The streptavidin-biotinylated protein complex was pelleted at 10,000 rpm for five minutes and washed four times. 50 μL of 1X Laemmli sample buffer was then added and the mixture heated in a 95°C heating block for 10 minutes to denature the protein and break the strepavidin-biotinylated protein bond. The streptavidin beads were pelleted on a table-top microcentrifuge and the supernatant quickly removed. An aliquot of the supernatant was taken for protein concentration measurement using the Bradford assay (Bio-Rad). 30 μg samples were resolved on SDS-PAGE and transferred to polyvinylidene difluoride membrane (Bio-Rad). Blots were then probed with CAIV polyclonal antibody (a kind gift from W. Sly) (1:2,000) and bound antibody was detected using ECL. The membrane was then stripped by using Re-blot plus strong antibody stripping solution (Chemicon) to remove CAIV antibody and blots were incubated with β-Actin polyclonal antibody (Sigma) (1:10,000) and developed by ECL. Films were scanned to produce digital images that were then assembled and labeled using Photoshop software.

Immunofluorescence

Cultured cells grown to confluence on coverslips were washed three to four times with warmed (37°C) PBS and fixed for 30 min in warmed PLP fixation solution (2% paraformaldehyde, 75 mM lysine, 10 mM sodium periodate, and 45 mM sodium phosphate, pH 7.4) on a rocker. After fixation, the cells were washed three to four times with PBS. Cells were blocked for 1 h in PBS that contained 0.2 % saponin, and bovine serum albumin, 5% goat serum, 0.01 % saponin, and 50 mM NH_4Cl. Rabbit polyclonal CAIV antibody and Rat monoclonal ZO-1 antibody (MAB1520, Chemicon) diluted 1:100 together in PBS/goat serum (1:1), was added onto coverslips and incubated for 1 h at room temperature or overnight at 4 °C. Coverslips were washed three times for 15 min in PBS that contained 0.01 % saponin. Secondary antibodies conjugated to Alexa 488 (NBC1) (Molecular Probes; 1:1000) and Alexa Fluor 594 (ZO-1) (Molecular Probes; 1:1000) were applied for 1hr at room temperature. Coverslips were washed with water and mounted with Prolong antifade medium according to the manufacturer's (Molecular Probes) instructions. Immunostaining was observed with a 40X oil objective lens using a standard epifluorescence microscope equipped with a CCD camera. A Bio-Rad 2000 laser scanning confocal microscope was used to obtain image stacks at 0.5 μm separation. Montages were created with Metamorph (Universal Imaging, West Chester, PA) software.

Microscope perfusion

For measurement of CO_2 and HCO_3^- transendothelial flux, cells were cultured to confluence on 13 mm diameter, 0.2 μm AnoDisc membranes. AnoDiscs were placed in a double-sided perfusion chamber designed for independent perfusion of the apical and basolateral sides [37]. The assembled chamber was placed on a water-jacketed (37°C) brass collar held on the stage of an inverted microscope (Nikon Diaphot 200) and viewed with a long working distance (2 mm) water-immersion objective (Nikon, X 40). Apical and basolateral compartments were connected to hanging syringes that contained Ringer solution in a Plexiglas warming box (37° C) using Phar-Med tubing. The flow of the perfusate (~0.5 ml/min) was achieved by gravity. Two independent eight-way valves were employed to select the desired perfusate for the apical and basolateral chambers. The composition of the standard HCO_3^--rich Ringer solution used throughout the study was (in mM) 150 Na^+, 4 K^+, 0.6 Mg^{2+}, 1.4 Ca^{2+}, 118 Cl^-, 1 HPO_4^-, 10 $HEPES^-$, 28.5 HCO_3^-, 2 gluconate, and 5 glucose, equilibrated with 5% CO_2 and pH adjusted to 7.50 at 37°C. HCO_3^--free Ringer solution (pH 7.50) was prepared by equimolar substitution of $NaHCO_3$ with sodium gluconate. Low-HCO_3^- Ringer solution (2.85 mM HCO_3^-, pH6.5) was prepared by replacing 25.65 mM $NaHCO_3$ with sodium gluconate.

Measurement of apparent CO_2 Flux

This was performed as previously described [33]. BCEC cultured onto permeable Anodisc filters were loaded with the pH-sensitive fluorescent dye BCECF. Intracellular pH (pH_i) was measured by obtaining fluorescence ratios (495 and 440 nM) of BCECF loaded cells at 1 s^{-1}. CO_2 flux from cell to apical compartment was determined using a constant pH protocol as described previously[30, 33]. Briefly, in the constant pH protocol the HCO_3^- rich Ringer on the apical side is replaced with a CO_2 and HCO_3^- free Ringer of the same pH (HEPES buffered). Under this protocol the initial pHi change is due to rapid CO_2 efflux (increase in pHi). The maximum slope of the pHi decrease is taken as an estimate of CO_2 flux.

Measurement of HCO_3^- Permeability

HCO_3^- permeability of the apical membrane was determined using a constant CO_2 protocol as described previously[33]. Under the constant CO_2 protocol, the HCO_3^- rich Ringer (28.5 mM, 5%CO_2, pH 7.5) is replaced with a low HCO_3^- (LB) solution (2.85 mM, 5% CO_2, pH 6.5). Under this protocol the initial pHi change is predominantly due to HCO_3^- efflux since there is

no CO_2 gradient. However there is a pH gradient that can contribute (~15%) to the initial pHi decrease [30].

Measurement of Transendothelial HCO_3^- Flux

These experiments were performed as previously described [33]. Briefly, BCEC cultured onto permeable Anodisc filters, perfused in a double-side chamber, were exposed to the standard HCO_3^--rich solution (5% CO_2/28.5 mM HCO_3^-, pH 7.5) on the basolateral and apical sides at 37°C. A low HCO_3^- solution (5% CO_2/2.85 mM HCO_3^{--}, pH 6.5) without Hepes buffer and containing 1μM BCECF free acid was then quickly exchanged on the apical side of the chamber and the exit tube on that side was clamped. The pH of the low HCO_3^- solution was estimated (1 Hz) at ~ 200 μm from the surface of the cells by measuring the fluorescence ratio of BCECF using the microscope fluorimeter. The pH of the low HCO_3^- solution rose from 6.5 and the initial rate of change over the first 20 seconds following clamping was estimated and served as an indirect measure of basolateral to apical (B to A) flux.

Measurement of Steady-State ΔpH

These experiments were performed as previously described[33] with minor modification. BCEC cultured to confluence on 0.2 μm Anopore membrane tissue culture inserts were washed with DMEM containing 2% bovine calf serum. 200 μl of this culture medium containing 1 μM BCECF free acid was placed on the apical side and 300 μl on the basolateral side. After 4 h in a standard 5% CO_2 incubator, 37°C, cultures were placed in a large glove box equilibrated with 5% CO_2, 37°C. 50 μl samples were taken from apical and basolateral sides with separate glass capillary tubes and both ends sealed with wax. The tubes were then taken to the microscope fluorimeter and the fluorescence ratio of BCECF was measured. The pH of each sample was then determined using a standard curve constructed using solutions of known pH that had been placed within capillary tubes. The difference in pH was calculated as, δpH = Apical pH - Basolateral pH. A positive ΔpH indicates relative apical alkalinization.

RESULTS

Data shown in figure 1 confirm the presence of CAIV in bovine corneal endothelial cells. Figure 1A shows PCR results indicating CAIV expression in bovine lung (positive control), fresh corneal endothelium and cultured corneal endothelial cells. Figure 1B shows western blot results using membrane preparations confirming protein expression in fresh and cultured endothelium. Molecular weight is estimated to be 35-40 kD, consistent with CAIV [38].

Indirect immunofluorescence was then performed to determine the membrane localization of CAIV. Figure 2A shows positive fluorescence for CAIV that is spread across the cell surface including the lateral junctions. There are also some concentrated caps of fluorescence near the cell center. This pattern of fluorescence is consistent with an apical localization. Figure 2B shows confocal fluorescence images using cells double stained for CAIV and the tight junction protein ZO-1. The CAIV fluorescence is either at the level of the ZO-1 fluorescence or more apical to ZO-1 consistent with the dome-shape of endothelial cells and confirming an apical location for CAIV.

To complement the effects of the extracellular carbonic anhydrase inhibitor benzolamide, we knock-downed CAIV expression using an siRNA approach. Figure 3A shows PCR results indicating significant knockdown at the mRNA level compared with control and siControl scrambled sequence. Figure 3B shows a representative western blot from control, siRNA, and siControl treated cells. The bar graph summarizes blot densities (n=3) indicating that knockdown was approximately 80%. This knockdown level is also reflected in immunofluorescence images from similarly treated cells (Figure 3C).

Previous studies showed that 10 μM benzolamide slowed apparent CO_2 fluxes across the apical membrane by ~25% and that this effect could be reversed by adding carbonic anhydrase to the apical bath [30], indicating that benzolamide was inhibiting an apical surface CA. Although this effect is small, it was reproducible. Furthermore, 10 μM benzolamide can cause corneal swelling [29], so we used 10 μM benzolamide as a reference for all our experiments in this study. Cells were loaded with the pH sensitive fluorescent dye BCECF and perfused on both apical and basolateral sides with bicarbonate-rich ringer. The apical perfusate was changed to bicarbonate free ringer, which induces an immediate efflux of CO_2 from the cells causing a rapid and significant cytosolic alkalinization. Figure 4A shows that 10 μM benzolamide, added to the apical side only, reduced apparent CO_2 fluxes by 23% (n=8), similar to that previously shown[30]. To test if CAIV knockdown by siRNA also affects apparent CO_2 flux, endothelial cells were seeded on Anodisc membranes and treated with siRNA for CAIV or siControl. Figure 4B shows that apparent CO_2 fluxes were also reduced by 21% in CAIV siRNA treated cells, relative to siControl treated cells. Furthermore, benzolamide had no effect on CO_2 fluxes in siRNA treated cells (data not shown). These experiments show that apparent apical CO_2 fluxes are reduced by CAIV knockdown and are comparable to benzolamide inhibition, consistent with apparent apical CO_2 fluxes facilitated by CAIV activity.

Carbonic anhydrases, including CAIV, can form transport metabolons with bicarbonate transporters to efficiently facilitate HCO_3^- fluxes [23, 24]. To test if this may be in place in corneal endothelium we measured apical HCO_3^- permeability in the presence of benzolamide or using CAIV siRNA treated cells. Cells were perfused with bicarbonate-rich ringer on apical and basolateral sides. Where indicated the apical perfusate was changed to low bicarbonate-constant CO_2 (LB) ringer. Under these conditions, the change in pHi is due to HCO_3^- efflux and the low pH_o of the LB ringer, which has a minor contribution[30]. Figure 5 shows that neither 10 μM benzolamide nor siRNA treated cells demonstrated a consistent inhibition of apical HCO_3^- permeability. On the other hand, 50 μM acetazolamide, which is cell permeable and blocks all CAs, reduced apparent HCO_3^- permeability by 40% (data not shown). These results suggest that CAIV is not part of a transport metabolon or other complex that facilitates HCO_3^- permeability.

A small transendothelial HCO_3^- flux in the basolateral to apical (B to A) direction can be demonstrated across corneal endothelial cell monolayers and shown to be inhibited by ouabain, siRNA knockdown of the basolateral $1Na^+$:$2HCO_3^-$ cotransporter[33], and ethoxyzolamide (a cell permeable CA inhibitor)[29]. To measure B to A HCO_3^- fluxes, cells were perfused in bicarbonate-rich ringer on the basolateral side and a low bicarbonate-low pH ringer on the apical side. Apical perfusion is stopped, outflow is clamped and the change in apical bath pH was measured. Figure 6A shows that 10 μM benzolamide, apical side only, had no effect on B to A HCO_3^- fluxes. Similarly, Figure 6B shows that CAIV siRNA treatment had no effect on B to A HCO_3^- fluxes. However, Figure 6 C shows that, as with HCO_3^- permeability, acetazolamide had a significant inhibitory effect on transendothelial HCO_3^- flux.

Lastly, we examined the effects of carbonic anhydrase inhibition and CAIV knockdown on steady-state ΔpH. Apical surface carbonic anhydrase activity could influence HCO_3^- fluxes, CO_2 fluxes, or apical surface buffering capacity. A reduction in ΔpH, defined as apical - basolateral pH after four hours, could be due to a reduction in net B to A HCO_3^- flux or a reduction in apical buffering capacity. Conversely, a reduction in net B to A CO_2 flux would increase ΔpH. Figure 7 shows that in control cultures, ΔpH was ~ +0.09 (apical side alkaline relative to basolateral), which is similar to what was previously reported [33]. Benzolamide, apical side only, reduced ΔpH to -0.03, significantly different from control, while the positive control, acetazolamide, reduced ΔpH to -0.10. In CAIV siRNA treated cells ΔpH was reduced to -0.03 from +0.06 pH units in siControl treated cells. These results are consistent with reduced HCO_3^- flux or reduced buffering capacity. Since benzolamide and CAIV siRNA do not affect

apical HCO_3^- permeability (figure 5) or B to A fluxes (figure 6), the results are best explained by reduced buffering capacity.

DISCUSSION

Membrane bound carbonic anhydrase activity in corneal endothelium was first demonstrated in mouse [39] and rat [15]. That this was CAIV was first indicated in corneal endothelium by indirect immunohistochemistry in paraffin embedded sections of postmortem human corneas suggesting both basolateral and apical membrane localization [16]. Another study showed CAIV expression was present in the rabbit corneal endothelium [17], but localization was not addressed. Here, we confirm expression of CAIV in bovine corneal endothelium, but localize it exclusively to the apical membrane using confocal microscopy.

Although carbonic anhydrase inhibitors (CAI) have been repeatedly shown to increase corneal thickness or slow stromal deturgescence of swollen corneas [1-3, 19], few studies have examined mechanistic details. Ethoxyzolamide, a cell permeant CAI, can reduce B to A HCO_3^- flux, however the effect of membrane impermeant CAIs on HCO_3^- flux were not tested [29]. Furthermore, 10 μM benzolamide or a dextran-linked CAI caused corneal swelling at about half the rate of cell permeant CAIs, indicating that CAIV and CAII have additive functions, and that CAIV has a role in endothelial function[29]. CAIV can facilitate apparent CO_2 flux when a CO_2 gradient is imposed across the apical membrane of bovine corneal endothelium (figure 4) [30]. As CO_2 moves across the plasma membrane it can be converted to HCO_3^- at the cell surface thereby maintaining a very steep cell to apical surface CO_2 gradient. This process is facilitated by CAIV. Inhibition of surface CA activity slows the conversion to HCO_3^- and thereby reduces the gradient for CO_2 efflux, slowing CO_2 efflux, and reducing the rate of pH_i change. On the basis of these results the hypothesis was put forth that net CO_2 flux from cytoplasm to anterior surface and then conversion to HCO_3^- could contribute to net basolateral to apical HCO_3^- flux [30]. Reducing CAIV expression by siRNA had a similar effect on apparent CO_2 flux (figure 4), consistent with the notion that CAIV can perform this function. One difficulty with this hypothesis is that under normal physiological conditions there is no established mechanism for net flux of CO_2 from cell to apical compartment as opposed to CO_2 diffusing from the cytoplasm equally in all directions. The hypothesis also predicts that inhibition of apical CAIV activity or knockdown of CAIV expression would slow the hydration of CO_2 at the apical surface and reduce an acidifying force. The steady-state pH experiments shown in figure 7 however, provide the opposite result indicating that a net cell to apical CO_2 flux is unlikely.

Recent studies have suggested that CAIV can form a transport metabolon by binding the extracellular loops of HCO_3^- transporters [24, 40]. As HCO_3^- translocates through the transporter protein from the cell to the extracellular surface, $[HCO_3^-]$ can build up at the membrane, but this is dissipated by conversion to CO_2, which is facilitated by CAIV. If this existed on the endothelial apical membrane, inhibition of CAIV activity or reduction of CAIV expression would reduce apparent HCO_3^- permeability and HCO_3^- flux. The absence of an effect on permeability or flux by benzolamide or in siRNA treated cells argues against an apical CAIV transport metabolon or other CAIV dependent facilitation of HCO_3^- flux. One assumption in interpreting these results is that CAIV activity remains rate limiting. This arises because the pH at the apical surface is lowered from 7.5 to 6.5, slowing the hydration of CO_2 by mass action. On the other hand, carbonic anhydrases raise the reaction rate by more than 10^5 [20], indicating that this effect is relatively minor.

CA activity is also associated with enhancing CO_2/HCO_3^- buffering capacity [26, 27]. Benzolamide has been shown to reduce cell surface buffering capacity in astrocytes [41, 42] and muscle fibers[43, 44]. Furthermore, we have found that cytosolic buffering capacity, measured

as δpHi/s in response to an ammonium pulse, is reduced 40% in the presence of acetazolamide in cultured corneal endothelial cells (unpublished results). Taken together, the results shown in figures 5-7 indicate that CAIV is not involved in facilitating HCO_3^- permeability, B to A HCO_3^- flux or CO_2 flux, but could influence apical surface buffering capacity. Confirmation of CAIV dependent buffering will require measurement of apical surface pH changes in response to acid or base loads.

How could a reduction in apical surface buffering capacity cause corneal swelling? Similarly, does reducing apical compartment buffering cause corneal swelling? There are several studies that show that replacing CO_2/HCO_3^- ringer's with phosphate buffered saline significantly reduce endothelial fluid transport [1-3]. Whereas this has been attributed to the removal of a "pump" substrate, it also significantly reduces buffering capacity. Interestingly, HCO_3^- poor ringer's with 50 mM added organic buffers can significantly increase endothelial transport [45, 46]. One possibility is that apical buffering facilitates lactic acid efflux. Lactate:H^+ cotransport is present at the apical membrane of corneal endothelium and a Na-dependent lactate transport is present at the basolateral membrane [47] (this is likely to be $1Na^+$:$2HCO_3^-$ cotransport in conjunction with lactate:H^+ cotransport). Thus CAIV may facilitate lactate fluxes across the apical membrane. Lactate is a potent osmolyte [48] and the cotransporter itself is thought to couple H_2O to the transport of lactate [49, 50]. Lactate fluxes can be facilitated by carbonic anhydrase activity in muscle [44, 51] and glia [42, 52]. Whether CA activity facilitates lactate transport across corneal endothelium remains to be tested.

In summary, CAIV is expressed in bovine corneal endothelium at the apical surface. Whereas inhibiting CAIV activity can reduce apparent apical CO_2 flux, this does not occur under steady-state conditions. CAIV does not have a significant role in facilitating apical HCO_3^- permeability or B to A HCO_3^- flux. CAIV can probably contribute to apical buffering, however further studies are needed to confirm this role and whether buffering contributes to endothelial function.

Acknowledgements

We would like to thank William Sly and Abdul Waheed for their kind gift of CAIV antibody.

This work was supported by grant EY08834 from the National Institute of Health

REFERENCES

1. Kuang K, Xu M, Koniarek J, Fischbarg J. Effects of ambient bicarbonate, phosphate and carbonic anhydrase inhibitors on fluid transport across rabbit endothelium. Exp Eye Res 1990;50:487–493. [PubMed: 2373152]
2. Hodson S, Miller F. The bicarbonate ion pump in the endothelium which regulates the hydration of rabbit cornea. J Physiol 1976;263:563–577. [PubMed: 828203]
3. Riley M, Winkler B, Czajkowski C, Peters M. The roles of bicarbonate and CO2 in transendothelial fluid movement and control of corneal thickness. Invest Ophthalmol Vis Sci 1995;36:103–112. [PubMed: 7822137]
4. Hull DS, Green K, Boyd M, Wynn HR. Corneal endothelium bicarbonate transport and the effect of carbonic anhydrase inhibitors on endothelial permeability and fluxes and corneal thickness. Invest Ophthalmol Vis Sci 1977;16:883–892. [PubMed: 908642]
5. Egan CA, Hodge DO, McLaren JW, Bourne WM. Effect of dorzolamide on corneal endothelial function in normal human eyes. Invest Ophthalmol Vis Sci 1998;39:23–29. [PubMed: 9430541]
6. Giasson CJ, Nguyen TQ, Boisjoly HM, Lesk MR, Amyot M, Charest M. Dorzolamide and corneal recovery from edema in patients with glaucoma or ocular hypertension. Am J Ophthalmol 2000;129:144–150. [PubMed: 10682965]

7. Kaminski S, Hommer A, Koyuncu D, Biowski R, Barisani T, Baumgartner I. Influence of dorzolamide on corneal thickness, endothelial cell count and corneal sensibility. Acta Ophthalmol Scand 1998;76:78–79. [PubMed: 9541439]
8. Wilkerson M, Cyrlin M, Lippa EA, et al. Four-week safety and efficacy study of dorzolamide, a novel, active topical carbonic anhydrase inhibitor. Arch Ophthalmol 1993;111:1343–1350. [PubMed: 8216014]
9. Wirtitsch MG, Findl O, Kiss B, Petternel V, Heinzl H, Drexler W. Short-term effect of dorzolamide hydrochloride on central corneal thickness in humans with cornea guttata. Arch Ophthalmol 2003;121:621–625. [PubMed: 12742838]
10. Konowal A, Morrison J, Brown S, et al. Irreversible Corneal Decompensation in Patients Treated With Tropical Dorzolamide. Am J Ophthalmol 1999;127:403–406. [PubMed: 10218692]
11. Tanimura H, Minamoto A, Narai A, Hirayama T, Suzuki M, Mishima HK. Corneal edema in glaucoma patients after the addition of brinzolamide 1% ophthalmic suspension. Jpn J Ophthalmol 2005;49:332–333. [PubMed: 16075340]
12. Conroy CW, Buck RH, Maren TH. The microchemical detection of carbonic anhydrase in corneal epithelia. Exp Eye Res 1992;55:637–640. [PubMed: 1483509]
13. Holthofer H, Siegal GJ, Tarkkanen A, Tervo T. Immunocytochemical localization of carbonic anhydrase, NaK-ATPase and the bicarbonate chloride exchanger in the anterior segment of the human eye. Acta Ophthalmologica 1991;69:149–154. [PubMed: 1651641]
14. Wistrand PJ, Schenholm M, Lonnerholm G. Carbonic anhydrase isoenzymes CA I and CA II in the human eye. Invest Ophthalmol Vis Sci 1986;27:419–428. [PubMed: 3081459]
15. Terashima H, Suzuki K, Kato K, Sugai N. Membrane-bound carbonic anhydrase activity in the rat corneal endothelium and retina. Japanese Journal of Opthamology 1995;40:142–153.
16. Wolfensberger TJ, Mahieu I, Carter ND, Hollande E, Bohnke M. Membrane-bound carbonic anhydrase (CA IV) in human corneal epithelium and endothelium. Klin Monatsbl Augenheilkd 1999;214:263–265. [PubMed: 10420360]
17. Cui W, Liu G, Liang R. Expression of carbonic anhydrase IV in rabbit corneal endothelial cells. Chinese medical journal 2002;115:1641–1644. [PubMed: 12609078]
18. Gottsch JD, Seitzman GD, Margulies EH, et al. Gene expression in donor corneal endothelium. Arch Ophthalmol 2003;121:252–258. [PubMed: 12583793]
19. Fischbarg J, Lim J. Role of cations, anions, and carbonic anhydrase in fluid transport across rabbit corneal endothelium. J Physiol 1974;241:647–675. [PubMed: 4215880]
20. Gutknecht J, Bisson MA, Tosteson FC. Diffusion of carbon dioxide through lipid bilayer membranes: effects of carbonic anhydrase, bicarbonate, and unstirred layers. J Gen Physiol 1977;69:779–794. [PubMed: 408462]
21. Purkerson JM, Schwartz GJ. The role of carbonic anhydrases in renal physiology. Kidney Int 2007;71:103–115. [PubMed: 17164835]
22. Mizumori M, Meyerowitz J, Takeuchi T, et al. Epithelial carbonic anhydrases facilitate PCO2 and pH regulation in rat duodenal mucosa. J Physiol 2006;573:827–842. [PubMed: 16556652]
23. McMurtrie HL, Cleary HJ, Alvarez BV, et al. The bicarbonate transport metabolon. J Enzyme Inhib Med Chem 2004;19:231–236. [PubMed: 15499994]
24. Sterling D, Alvarez BV, Casey JR. The extracellular component of a transport metabolon. Extracellular loop 4 of the human AE1 Cl-/HCO3- exchanger binds carbonic anhydrase IV. J Biol Chem 2002;277:25239–25246. [PubMed: 11994299]
25. Sterling D, Brown NJ, Supuran CT, Casey JR. The functional and physical relationship between the DRA bicarbonate transporter and carbonic anhydrase II. Am J Physiol Cell Physiol 2002;283:C1522–1529. [PubMed: 12372813]
26. De Marchi S, Cecchin E. Severe metabolic acidosis and disturbances of calcium metabolism induced by acetazolamide in patients on haemodialysis. Clin Sci (Lond) 1990;78:295–302. [PubMed: 2156649]
27. Leaf DE, Goldfarb DS. Mechanisms of action of acetazolamide in the prophylaxis and treatment of acute mountain sickness. J Appl Physiol 2007;102:1313–1322. [PubMed: 17023566]
28. Bonanno JA, Srinivas SP, Brown M. Effect of acetazolamide on intracellular pH and bicarbonate transport on bovine corneal endothelium. Exp Eye Res 1995;60:425–434. [PubMed: 7789422]

29. Diecke FP, Wen Q, Sanchez JM, Kuang K, Fischbarg J. Immunocytochemical localization of Na+-HCO3- cotransporters and carbonic anhydrase dependence of fluid transport in corneal endothelial cells. Am J Physiol Cell Physiol 2004;286:C1434–1442. [PubMed: 14960417]
30. Bonanno J, Guan Y, Jelamskii S, Kang X. Apical and basolateral CO_2-HCO_3^- permeability in cultured bovine corneal endothelial cells. Am J Physiol 1999;277:C545–C553. [PubMed: 10484341]
31. Bonanno JA, Giasson C. Intracellular pH regulation in fresh and cultured bovine corneal endothelium. I. Na/H exchange in the absence and presence of HCO_3- Invest Ophthalmol Vis Sci 1992;33:3058–3067. [PubMed: 1328110]
32. Xie Q, Zhang Y, Cai Sun X, Zhai C, Bonanno JA. Expression and functional evaluation of transient receptor potential channel 4 in bovine corneal endothelial cells. Exp Eye Res 2005;81:5–14. [PubMed: 15978249]
33. Li J, Sun XC, Bonanno JA. Role of NBC1 in apical and basolateral HCO3- permeabilities and transendothelial HCO3- fluxes in bovine corneal endothelium. Am J Physiol Cell Physiol 2005;288:C739–746. [PubMed: 15548570]
34. Zhang Y, Li J, Xie Q, Bonanno JA. Molecular expression and functional involvement of the bovine calcium-activated chloride channel 1 (bCLCA1) in apical HCO3- permeability of bovine corneal endothelium. Exp Eye Res 2006;83:1215–1224. [PubMed: 16899243]
35. Yang H, Mergler S, Sun X, et al. TRPC4 knockdown suppresses epidermal growth factor-induced store-operated channel activation and growth in human corneal epithelial cells. J Biol Chem 2005;280:32230–32237. [PubMed: 16033767]
36. Tan-Allen KY, Sun XC, Bonanno JA. Characterization of adenosine receptors in bovine corneal endothelium. Exp Eye Res 2005;80:687–696. [PubMed: 15862176]
37. Bonanno JA, Yi G, Kang XJ, Srinivas SP. Reevaluation of Cl-/HCO3- exchange in cultured bovine corneal endothelial cells. Invest Ophthalmol Vis Sci 1998;39:2713–2722. [PubMed: 9856782]
38. Okuyama T, Sato S, Zhu XL, Waheed A, Sly WS. Human carbonic anhydrase IV: cDNA cloning, sequence comparison, and expression in COS cell membranes. Proc Natl Acad Sci U S A 1992;89:1315–1319. [PubMed: 1311094]
39. Ridderstrale Y, Wistrand PJ, Brechue WF. Membrane-associated CA activity in the eye of CA II-deficient mouse. Invest Ophthalmol Vis Sci 1994;35:2577–2584. [PubMed: 8163345]
40. Alvarez BV, Loiselle FB, Supuran CT, Schwartz GJ, Casey JR. Direct extracellular interaction between carbonic anhydrase IV and the human NBC1 sodium/bicarbonate co-transporter. Biochemistry 2003;42:12321–12329. [PubMed: 14567693]
41. Shah GN, Ulmasov B, Waheed A, et al. Carbonic anhydrase IV and XIV knockout mice: roles of the respective carbonic anhydrases in buffering the extracellular space in brain. Proc Natl Acad Sci U S A 2005;102:16771–16776. [PubMed: 16260723]
42. Svichar N, Esquenazi S, Waheed A, Sly WS, Chesler M. Functional demonstration of surface carbonic anhydrase IV activity on rat astrocytes. Glia 2006;53:241–247. [PubMed: 16265666]
43. Kaila K, Saarikoski J, Voipio J. Mechanism of action of GABA on intracellular pH and on surface pH in crayfish muscle fibres. J Physiol 1990;427:241–260. [PubMed: 1698980]
44. Saarikoski J, Kaila K. Simultaneous measurement of intracellular and extracellular carbonic anhydrase activity in intact muscle fibres. Pflugers Archive 1992;421:357–363. [PubMed: 1408660]
45. Doughty MJ, Maurice D. Bicarbonate sensitivity of rabbit corneal endothelium fluid pump in vitro. Invest Ophthalmol Vis Sci 1988;29:216–223. [PubMed: 3123416]
46. Doughty MJ, Newlander K, Olejnik O. Effect of bicarbonate-free balanced salt solutions on fluid pump and endothelial morphology of rabbit corneas in-vitro. J Pharm Pharmacol 1993;45:102–109. [PubMed: 7680710]
47. Giasson C, Bonanno JA. Facilitated transport of lactate by rabbit corneal endothelium. Exp Eye Res 1994;59:73–81. [PubMed: 7835399]
48. Klyce SD. Stromal lactate accumulation can account for corneal oedema osmotically following epithelial hypoxia in the rabbit. J Physiol 1981;321:49–64. [PubMed: 7338822]
49. Hamann S, Kiilgaard JF, la Cour M, Prause JU, Zeuthen T. Cotransport of H+, lactate, and H2O in porcine retinal pigment epithelial cells. Exp Eye Res 2003;76:493–504. [PubMed: 12634113]
50. Loo DD, Wright EM, Zeuthen T. Water pumps. J Physiol 2002;542:53–60. [PubMed: 12096049]

51. Wetzel P, Hasse A, Papadopoulos S, Voipio J, Kaila K, Gros G. Extracellular carbonic anhydrase activity facilitates lactic acid transport in rat skeletal muscle fibres. J Physiol 2001;531:743–756. [PubMed: 11251055]

52. Svichar N, Chesler M. Surface carbonic anhydrase activity on astrocytes and neurons facilitates lactate transport. Glia 2003;41:415–419. [PubMed: 12555208]

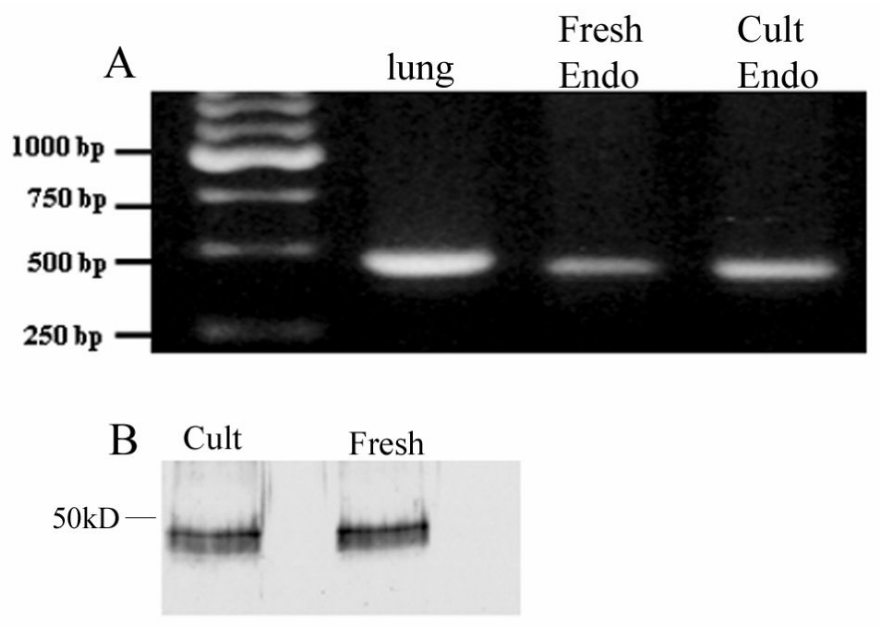

Figure 1.
A. RT-PCR result for CAIV from bovine lung (positive control), fresh bovine corneal endothelium, and cultured bovine corneal endothelium. B, Western blot of membrane preparations from cultured and fresh bovine corneal endothelium.

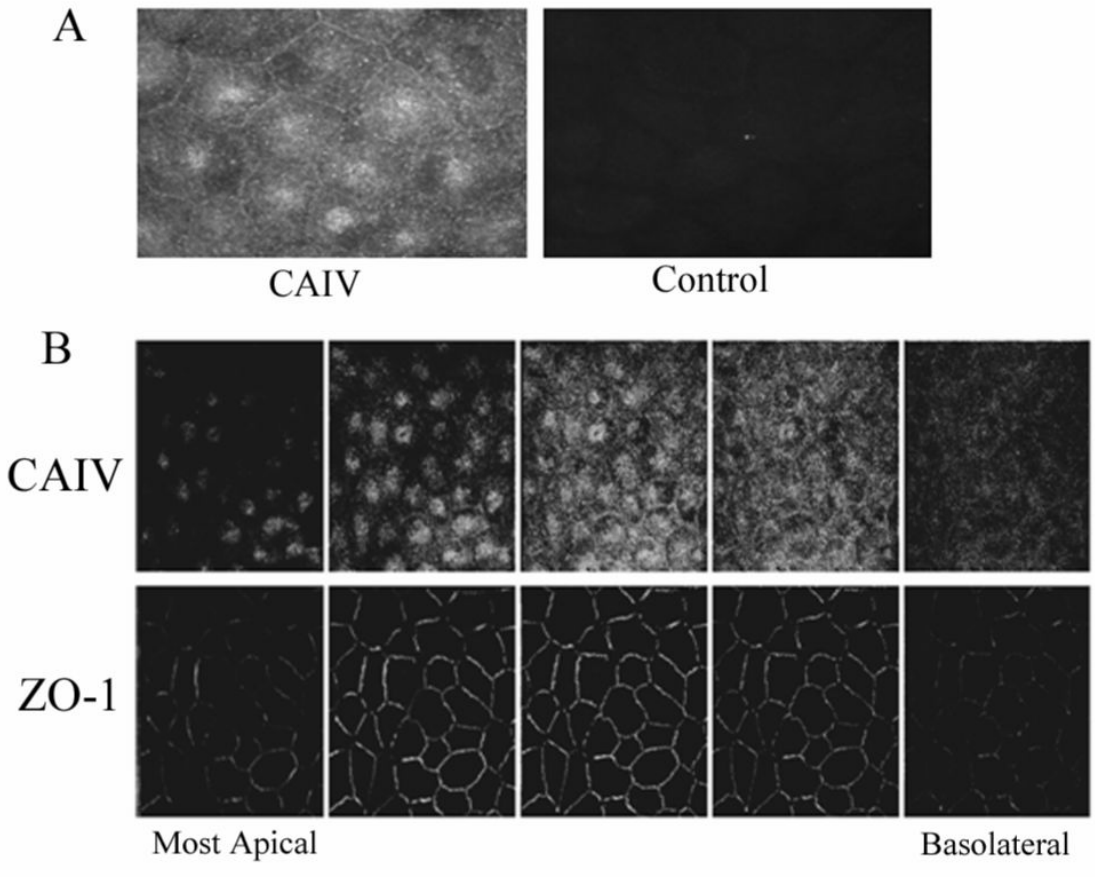

Figure 2.
Immunofluorescence localization of CAIV in bovine corneal endothelium. A. fresh corneal endothelium; left, positive surface staining; right, control-absence of primary antibody. B. Confocal montage of cultured corneal endothelial cells stained for CAIV and ZO-1. Leftmost image pair is the most apical section. Z-axis separation between images is 0.5 μm. The five images represent a distance of 2.5 μm. CAIV fluorescence is either apical to or coincident with ZO-1.

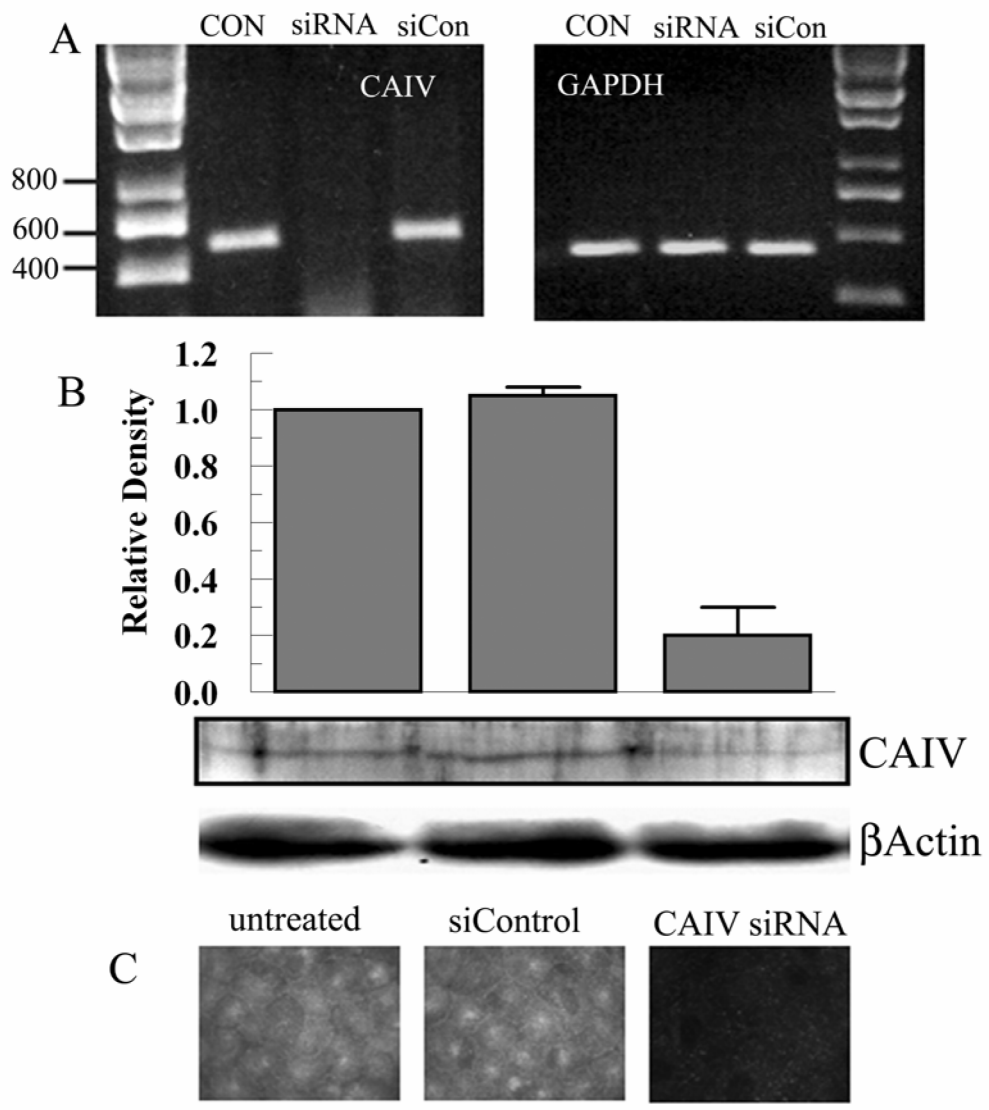

Figure 3.

siRNA knockdown of CAIV. A. Semi-quantitative PCR for CAIV and GAPDH (Glyceraldehyde phosphate dehydrogenase) using untreated, siRNA (20 nM), and siControl (20 nM) treated cultured endothelial cells. B. Western blot for CAIV and βactin using siRNA, and siControl treated cultured endothelial cells. Bar graph shows relative density (referenced to actin) from 3 paired experiments. C. Immunofluorescence micrograph for CAIV.

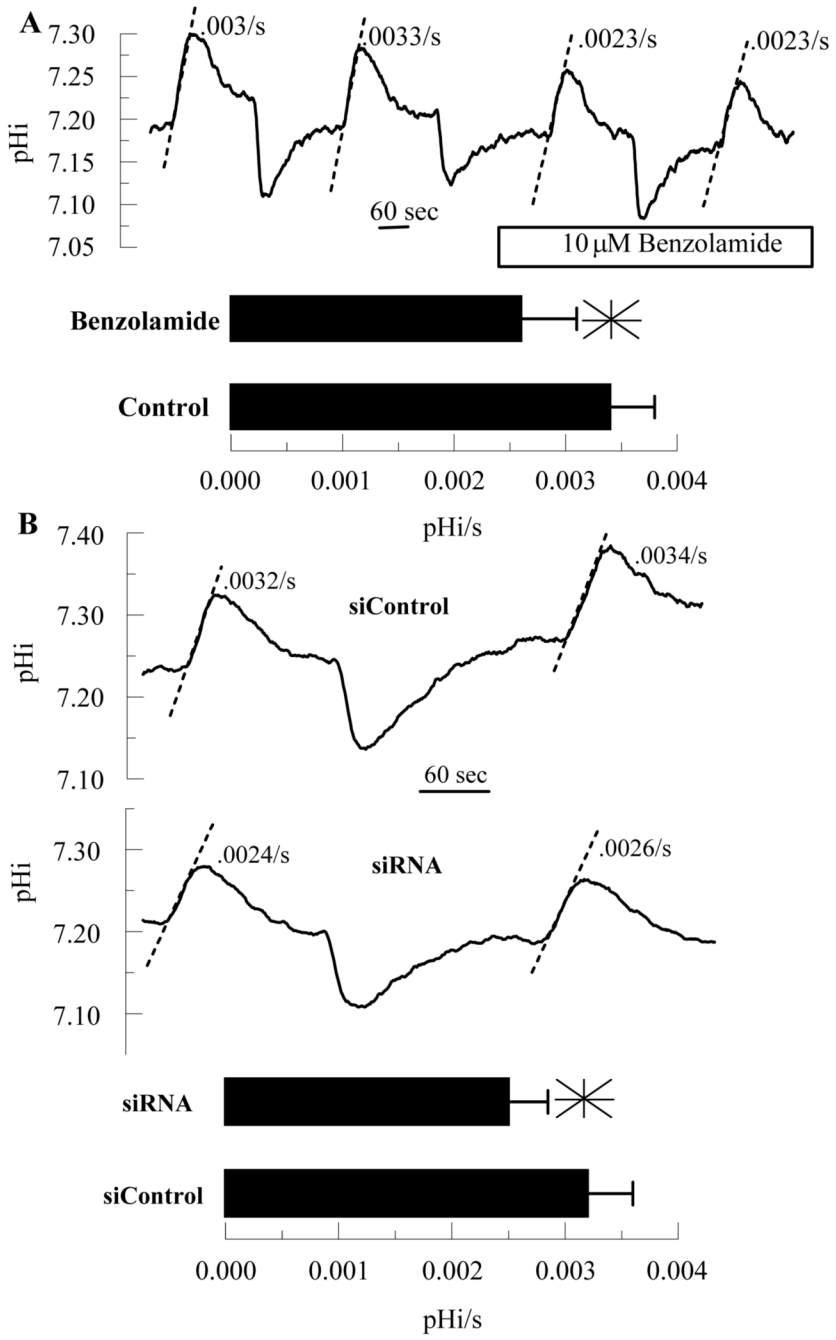

Figure 4.

Effect of Benzolamide and CAIV siRNA on Apparent CO_2 fluxes. BCECF loaded endothelial cells were perfused in a two-sided chamber. The alkalinizations were due to changing the apical perfusate to a CO_2/HCO_3^- free ringer. The dashed lines illustrate the estimated rate (pH_i/s). A. This was performed twice in the absence and then in the presence of 10 μM benzolamide on the apical side. Bar graph shows mean rates and SD (n=12 anodiscs); *significantly lower than control ($p<0.05$, paired t-test). B. Representative comparisons of siControl and CAIV treated cells. Bar graph shows mean rates and SD (n=10 anodiscs); *significantly lower than control ($p<0.05$, indendent t-test).

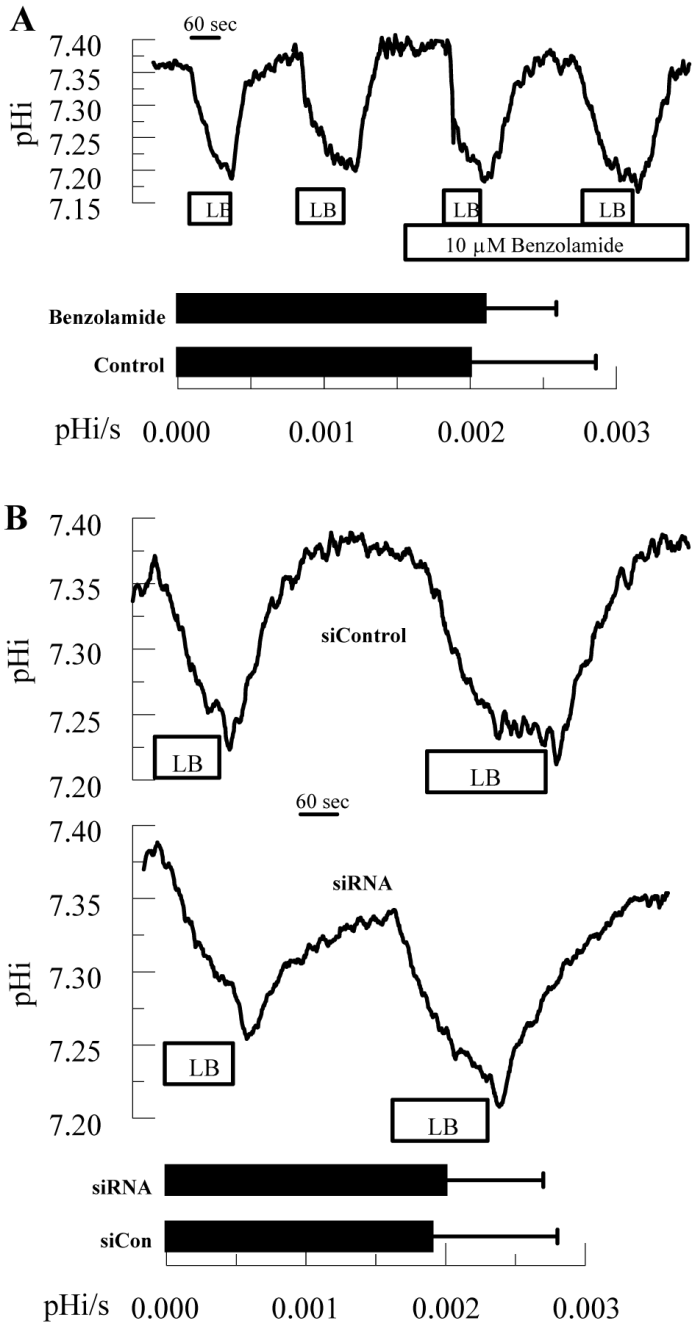

Figure 5.

Effect of Benzolamide and CAIV siRNA on apical HCO_3^- Permeability. BCECF loaded endothelial cells were perfused in a two-sided chamber. Where indicated the apical ringer was changed from bicarbonate-rich to low-bicarbonate ringer (LB) to determine the maximal rate of acidification. A. This was performed twice in the absence and then in the presence of 10 μM benzolamide on the apical side. Bar graph shows mean rates and SD (n=12 anodiscs). B. Representative comparisons of siControl and CAIV treated cells. Bar graph shows mean rates and SD (n=10 anodiscs).

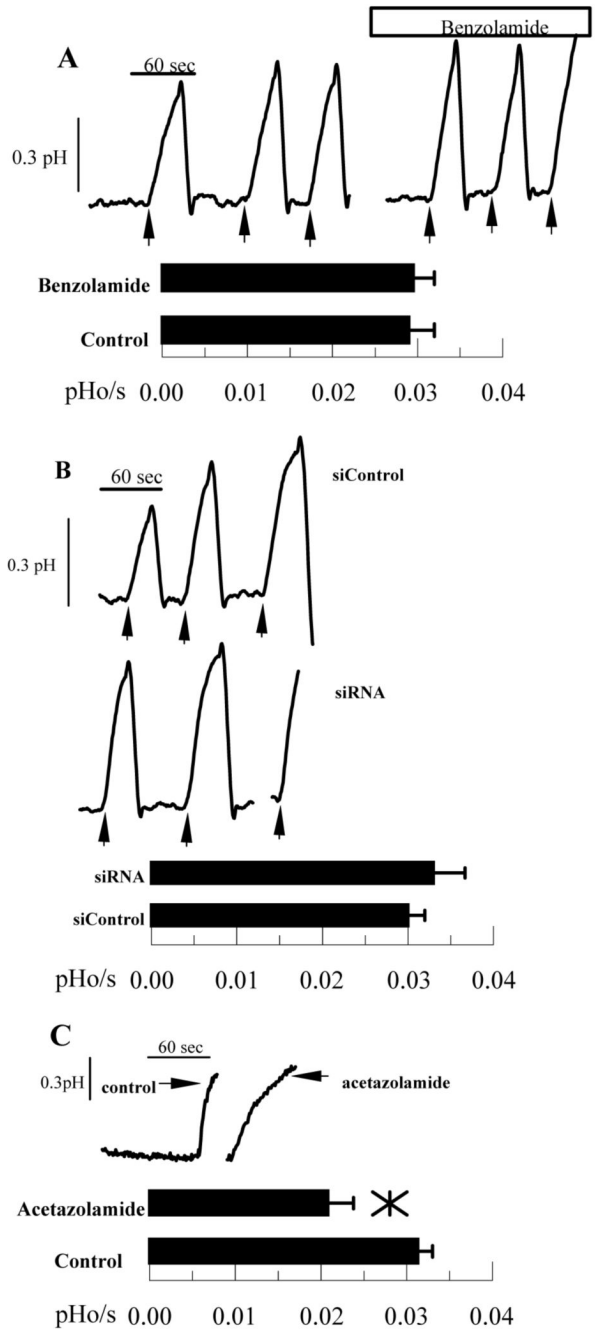

Figure 6.

Effect of Benzolamide and CAIV siRNA on basolateral to apical HCO_3^- Flux. Endothelial cells were perfused with bicarbonate-rich ringer in a two-sided chamber. The apical ringer was then changed to LB ringer (pH 6.5) containing 1 μM BCECF free acid to measure apical ringer pH. Arrows indicate when apical perfusion was stopped and apical outflow clamped. A. This was performed three times in the absence and then in the presence of 10 μM benzolamide on the apical side. Bar graph shows mean rates and SD (n=12 anodiscs). B. Representative comparisons of siControl and CAIV treated cells. Bar graph shows mean rates and SD (n=10 anodiscs). C. Positive control; representative traces showing decreased HCO_3^- flux with 50 μM acetazolamide (n=4) on both basolateral and apical sides.

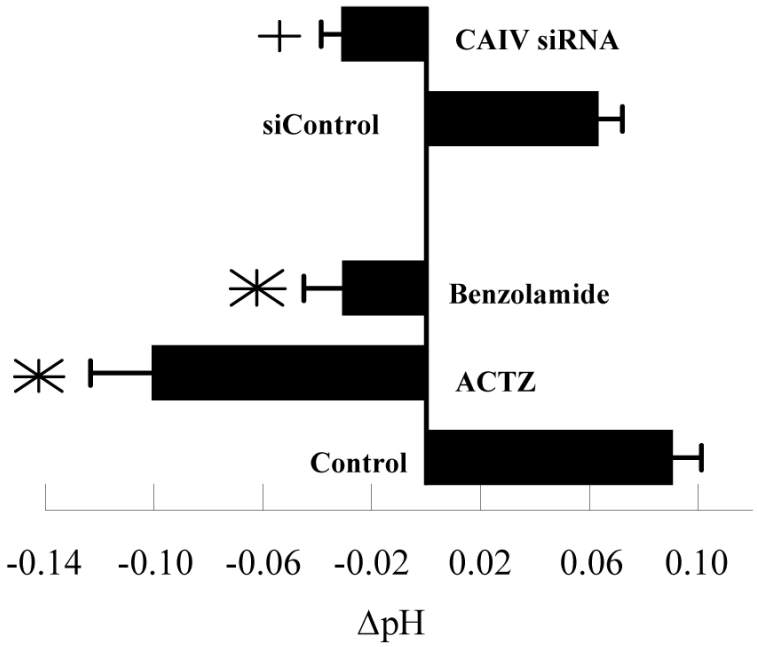

Figure 7.
Effect of Benzolamide and CAIV siRNA on steady-state ΔpH (apical-basolateral pH) after 4 hours. *significantly different from control ($p<0.05$, $n=6$); +significantly different from siControl. Error bars indicate SD.